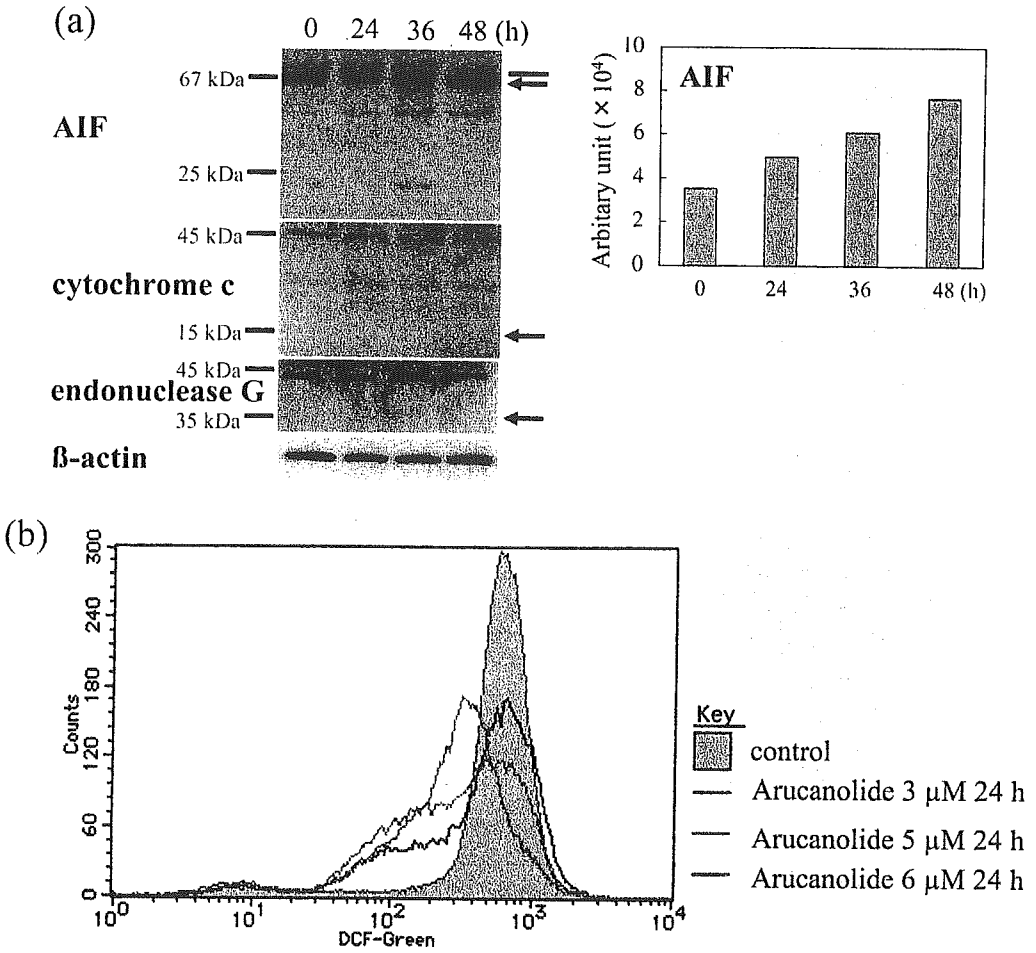

Fig. 4. Arucanolide-induced cell death in HL60. a: Activation of AIF, cytochrome c, and endonuclease G after the treatment with 6 μM arucanolide examined by Western blot analysis. b: Mitochondrial membrane potential after treatment with 3, 5, or 6 μM arucanolide. The relative fluorescence intensity of Mito-Tracker Orange was measured by flow cytometry. The patterns of fluorescence intensity of Mito-Tracker Green were almost similar in the samples tested. c: Time course of Bcl-2 and BAX mRNA expression after the treatment with 6 μM arucanolide.

examined the activation of NF-κB in arucanolide-induced apoptosis (Fig. 5). When apoptotic stimuli including TNF-α cause phosphorylation of IκB, NF-κB is activated and translocates into nuclei. In our study, Western blot analysis showed that the level of phosphorylated IκB was unchanged (Fig. 5a). When the cells transfected with pNF-κB-SEAP vector were exposed to TNF-α, the cis-element for NF-κB was functioning and the mRNA and protein expression of alkaline phosphatase was increased (11, 12). We examined the SEAP activity in the culture medium after TNF-α treatment in the presence of parthenolide or arucanolide. Although parthenolide prevented the increase in SEAP activity, arucanolide did not (Fig. 5b), indicating that arucanolide did not block activation of NF-κB.

Effect of arucanolide on MAP kinases

We examined the activation of MAP kinases (Fig. 6) in arucanolide-induced apoptosis. The level of p-p44/42 MAP kinase decreased within 4 h after the arucanolide treatment (Fig. 6). p-JNK was transiently increased at

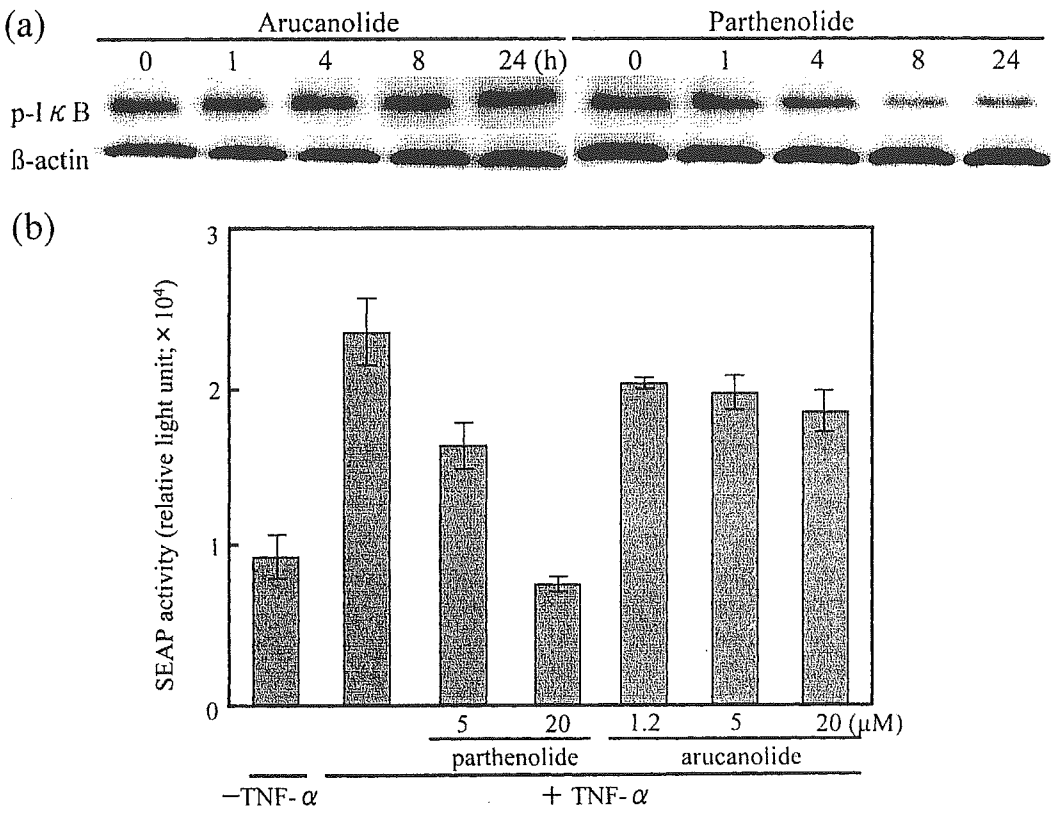

Fig. 5. NF-κB signaling in arucanolide-induced cell death. a: Phosphorylated form of IκB in HL60 cells examined by Western blot analysis compared with those in parthnolide-treated cells. b: Secreted alkaline phosphatase (SEAP) activety in parthenolide- and arucanolide-treated HeLa cells. The method is described in Materials and Methods.

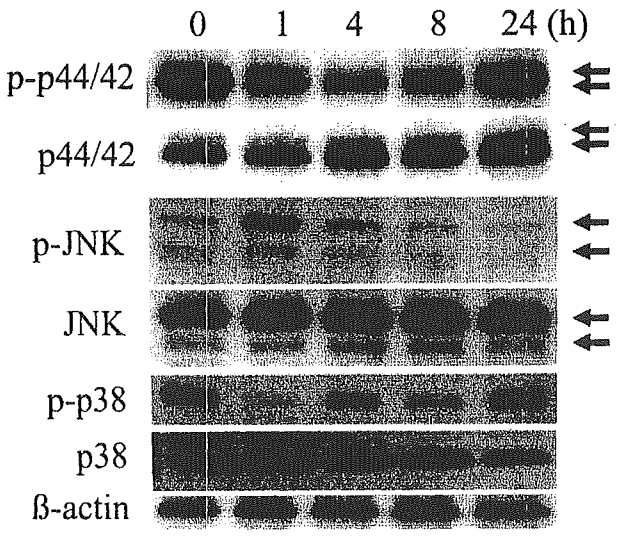

Fig. 6. Death-associated MAP kinase signaling of arucanolide-induced cell death in HL60 cells. p44/42 MAP kinase, p-p44/42 MAP kinase, JNK, p-JNK, p38, and p-p38 were examined by Western blot analysis.

1 h after the treatment (Fig. 6). p-p38 was transiently decreased at 1 h after treatment (Fig. 6). p44/42 MAP kinase has been known to inhibit apoptosis by phosphorylating Bad (Ser 112/155) (15 – 18); phosphorylated Bad (Ser 155) does not dimerize with Bcl-xL, leading to inhibition of apoptosis (18, 19). We did not observe significant changes in phosphorylated Bad (Ser 112) and Bcl-xL levels after the arucanolide treatment (data not shown).

Discussion

This study was undertaken to explore biological activities of the sesquiterpene lactones in *Calea urticifolia*. Six sesquiterpene lactones, including parthenolide were examined for effects on cytotoxicity. All compounds tested exhibited significant cytotoxic activity in HL60 and SW480 cells. Especially, arucanolide exerted a marked cytotoxic effect at less than 10 μM against both cell lines and its cytotoxic activity is greater than parthenolide, which has been reported to have a potent anticancer effect (20 – 22).

Parthenolide, which is one of the most important

active ingredients in the herb European and American feverfew (*Tanacetum parthenium*), has been shown to inhibit NF-κB (3 – 5). Moreover, parthenolide induces apoptosis through the activation of caspase-3 and necrosis through the disruption of the cell membrane in HL60 cells (20, 21). Parthenolide has been thought to be one of the promising chemotherapeutic agents because parthenolide triggers apoptosis in sarcomatoid hepatocellular carcinoma SH-J1 cells and also other hepatoma cell lines at low doses of 5 – 10 μM (22). In the present study, we have found that arucanolide had a more potent cytotoxic effect compared to parthenolide as reflected in IC_{50}s against HL60 or SW480 cell lines. Furthermore, we found that the cytotoxicity was due to apoptosis mediated by loss of mitochondrial membrane potential and the concurrent AIF release in HL60 cells. Many chemopreventive agents act through induction of apoptosis which would result in inhibition of the carcinogenesis process. During the last several years, it has become increasingly clear that mitochondria play a major rate-limiting role in apoptosis. The decision /effecter phase of the apoptotic process converges on mitochondria, where permeabilization of mitochondrial membranes is triggered; and apoptosis inducing factors such as cytochrome c, AIF, and endonuclease G are released. It has been reported that released AIF was gathered around the nuclei in the cytoplasm and partly translocated into nuclei after the treatment of the apoptogenic dolichyl monoposphate in U937 cells and that both caspase-3 and 8 inhibitors blocked the DNA fragmentation (23). AIF causes chromatin condensation and large scale DNA fragmentation of approximately 50 kb (24). Surely, it is not clear whether AIF directly contributes to DNA ladder formation. In our present study, it was shown that arucanolide-induced apoptosis was mediated by the mitochondrial pathway, and that the released AIF level was time-dependently increasing after exposure to arucanolide. Accordingly, our data raise the possibility that AIF, but not caspases, may play a crucial role in DNA ladder formation by one or more yet undefined mechanisms. It was also to be noted that the mechanism of apoptosis induced by arucanolide was different from that of parthenolide. Parthenolide inhibits the activation of NF-κB (3 – 5), but arucanolide did not affect NF-κB.

Traditionally, sesquiterpene lactones have been used as folk medicines because of their various bioactivities. For example, Tenulin and Helenalin were reported to have an ability to inhibit of DNA synthesis of Ehrlich ascites cells and P-388 cells (25 – 27). Artemisinin, a sesquiterpene lactone with an endoperoxide group, was used as an anti-malarial drug and was effective against both drug-resistant and cerebral malaria-causing stains of *Plasmodium falciparum* (28). Artemisinin inhibits nitric oxide synthesis in cytokine-stimulated human astrocytoma T67 cells through the inhibition of NF-κB activation (29). Costunolide, a naturally occurring sesquiterpene lactone, reduced the frequency of colonic aberrant crypt foci induced by azoxymethane (30) and was reported to cause a strong growth inhibition against HL60 cells with apoptotic chromatin condensation (31). Furthermore, costunolide suppresses gene expression of hepatitis B virus surface antigen in human hepatoma cells (32).

Parthenolide has been shown to improve endotoxic shock by reducing plasma nitrate/nitrite level and to reduce lung neutrophil infiltration in the rat sepsis model because it attenuated inducible nitric oxide synthase by inhibiting NF-κB activity (33, 34). Patel et al. reported that parthenolide mimicked the effects of IκB-α by inhibiting DNA binding activity of NF-κB and manganese superoxide dismutase (Mn-SOD) expression, which leads to an enhancing paclitaxel-induced apoptosis of breast cancer cells (35). It was also reported that apoptosis by germacranolides such as tatridine A diacetate and ineupatorolide A was accompanied by an early release of cytochrome c from mitochondria, followed by both activation of caspase-3 and fragmentation of poly (ADP-ribose) polymerase-1 (36). Thus, the mechanism of arucanolide-induced apoptosis was found to be clearly distinct from that of other sesquiterpene lactones.

The levels of p-p44/42, p-JNK, and p-p38 were changed within 24 h after the arucanolide-treatment; however, their levels were restored over 24-h after treatment. We did not conclude that these changes were related to the apoptotic signals. We are making ongoing investigations about this.

IC_{50} of arucanolide in mitogen-stimulated normal peripheral blood lymphocytes was observed at 2.3 μM, but that of parthenolide was 1.1 μM (Table 1b), suggesting that arucanolide is more plausible than parthenolide for application as a chemopreventive agent.

As to the structure-activity relationship of germacranolides tested, the cytotoxic activity observed in the present study was as follows: arucanolide > (parthenolide) > calealactone A > 2,3-epoxy-juanislamin > 2,3-epoxy-calealactone A = calealactone B. The presence of a double bond at C-2 and C-3 seems to be preferable to an epoxyl group. Esterification sometimes enhances the bioactivity as observed for aconitine. Arucanolide is esterified at C-8 and C-9 with two organic acids, which influences the cytotoxic activity. Hydrogenation of a side chain moiety often reduces the bioactivity, which is applied to a 2-methylbutylric acid moiety at C-9 in calealactone A and 2,3-epoxy-calealactone A. The carbon chain length of the organic acid is also important.

As seen in arucanlide, the acetyl group at C-8 may be more efficient in terms of the activity than a 2-methylacryl group.

We would conclude that arucanolide is more advantageous as a chemopreventive agent than parthenolide. Further experiments are required to assess the anticancer effect of arucanolide in an animal model and also to define the detailed mechanisms at the molecular level, which are under current progress in our laboratory.

References

1 Yamada M, Matsuura M, Suzuki J, Kurosawa C, Hasewaga N, Ubukata M, et al. Germacrolides from *Calea urticifolia*. Phytochemistry. 2004;65:3107–3111.

2 Hoffmann JJ, Torrance SJ, Widehopf RM, Cole JR. Cytotoxic agents from Michelia champaca and Talauma ovata: parthenolide and costunolide. J Pharm Sci. 1977;66:883–884.

3 Bork PM, Schmitz ML, Kuhnt M, Escher C, Heinrich M. Sesquiterpene lactone containing Mexican Indian medicinal plants and pure sesquiterpene lactones as potent inhibitors of transcription factor NF-κB. FEBS Lett. 1997;402:85–90.

4 Hehner SP, Heinrich M, Bork PM, Vogt M, Ratter F, Lehmann V, et al. Sesquiterpene lactones specifically inhibit activation of NF-κB by preventing the degradation of IκB-α and IκB-β. J Biol Chem. 1998;273:1288–1297.

5 Hehner SP, Hofmann TG, Droge W, Schmitz ML. The anti-inflammatory sesquiterpene lactone parthenolide inhibits NF-κB by targeting the IκB kinase complex. J Immunol. 1999;163:5617–5623.

6 Huang XJ, Wiernik PH, Klein RS, Gallagher RE. Arsenic trioxide induces apoptosis of myeloid leukemia cells by activation of caspases. Med Oncol. 1999;16:58–64.

7 Cai X, Shen YL, Zhu Q, Jia PM, Yu Y, Zhou L, et al. Arsenic trioxide-induces apoptosis and differentiation are associated respectively with mitochondrial transmembrane potential collapse and retinoic acid signaling pathway in acute promyelocytic leukemia. Leukemia. 2000;14:262–270.

8 Akao Y, Tsujimoto Y, Finan J, Nowell PC, Croce CM. Molecular characterization of a t(11;14)(q23;q32) chromosome translocation in a B-cell lymphoma. Cancer Res. 1990;50:4856–4859.

9 Akao Y, Otsuki Y, Kataoka S, Ito Y, Tsujimoto Y. Multiple subcellular localization of bcl-2: detection in nuclear outer membrane, endoplasmic reticulum membrane, and mitochondrial membranes. Cancer Res. 1994;54:2468–2471.

10 Nakagawa Y, Akao Y, Morikawa H, Hirata I, Katsu K, Naoe T, et al. Arsenic trioxide-induced apoptosis through oxidative stress in cells of colon cancer cell lines. Life Sci. 2002;70:2253–2269.

11 Kain SR. Use of secreted alkaline phosphatase as a reporter of gene expression in mammalian cells. Methods Mol Biol. 1997;63:49–60.

12 Berger J, Hauber J, Hauber R, Geiger R, Cullen BR. Secreted placental alkaline phosphatase: a powerful new quantitative indicator of gene expression in eukaryotic cells. Gene. 1988;66:1–10.

13 Hall CV, Jacob PE, Ringold GM, Lee F. Expression and regulation of *Escherichia coli* lacZ gene fusions in mammalian cells. J Mol Appl Genet. 1983;2:101–109.

14 Tsujimoto Y, Shimizu S. bcl-2 family: Life-or-death switch. FEBS Lett. 2000;466:6–10.

15 Chen RH, Sarnecki C, Blenis J. Nuclear localization and regulation of erk- and rsk-encoded protein kinases. Mol Cell Biol. 1992;12:915–927.

16 Bonni A, Brunet A, West AE, Datta SR, Takasu MA, Greenberg ME. Cell survival promoted by the Ras-MAPK signaling pathway by transcription-dependent and -independent mechanisms. Science. 1999;286:1358–1362.

17 Zha J, Harada H, Yang E, Jockel J, Korsmeyer SJ. Serine phosphorylation of death agonist BAD in response to survival factor results in binding to 14-3-3 not BCL-X(L). Cell. 1996;87:619–628.

18 Lizcano JM, Morrice N, Cohen P. Regulation of BAD by cAMP-dependent protein kinase is mediated via phosphorylation of a novel site, Ser155. Biochem J. 2000;15:547–557.

19 Tan Y, Demeter MR, Ruan H, Comb MJ. BAD Ser-155 phosphorylation regulates BAD/Bcl-XL interaction and cell survival. J Biol Chem. 2000;275:25865–25869.

20 Pozarowski P, Halicka DH, Darzynkiewicz Z. Cell cycle effects and caspase-dependent and independent death of HL-60 and Jurkat cells treated with the inhibitor of NF-κB parthenolide. Cell Cycle. 2003;2:377–383.

21 Pozarowski P, Halicka DH, Darzynkiewicz Z. NF-κB inhibitor sesquiterpene parthenolide induces concurrently atypical apoptosis and cell necrosis: difficulties in identification of dead cells in such cultures. Cytometry. 2003;54A:118–124.

22 Wen J, You KR, Lee SY, Song CH, Kim DG. Oxidative stress-mediated apoptosis. The anticancer effect of the sesquiterpene lactone parthenolide. J Biol Chem. 2002;277:38954–38964.

23 Yasugi E, Kumagai T, Nishikawa Y, Okuma E, Saeki K, Oshima M, et al. Involvement of apoptosis-inducing factor during dolichyl monophosphate-induced apoptosis in U937 cells. FEBS Lett. 2000;480:197–200.

24 Lorenzo HK, Susin SA, Penningen J, Kroemer G. Apoptosis inducing factor (AIF): a phylogenetically old, caspase-independent effector of cell death. Cell Death Differ. 1999;6:516–524.

25 Hall IH, Lee KH, Mar EC, Starnes CO, Waddell TG. Antitumor agents. 21. A proposed mechanism for inhibition of cancer growth by tenulin and helenalin and related cyclopentenones. J Med Chem. 1977;20:333–337.

26 Williams WL Jr, Hall IH, Grippo AA, Oswald CB, Lee KH, Holbrook DJ, et al. Inhibition of nucleic acid synthesis in P-388 lymphocytic leukemia tumor cells by helenalin and bis(helenalinyl)malonate in vivo. J Pharm Sci. 1988;77:178–184.

27 Hall IH, Grippo AA, Holbrook DJ, Roberts G, Lin HC, Kim HL, et al. Role of thiol agents in protecting against the toxicity of helenalin in tumor-bearing mice. Planta Med. 1989;55:513–517.

28 Abdin MZ, Israr M, Rehman RU, Jain SK. Artemisinin, a novel antimalarial drug: biochemical and molecular approaches for enhanced production. Planta Med. 2003;69:289–299.

29 Aldieri E, Atragene D, Bergandi L, Riganti C, Costamagna C, Bosia A, et al. Artemisinin inhibits inducible nitric oxide synthase and nuclear factor NF-κB activation. FEBS Lett. 2003;552:141–144.

30 Kawamori T, Tanaka T, Hara A, Yamahara J, Mori H. Modifying effects of naturally occurring products on the development of colonic aberrant crypt foci induced by azoxymethane in F344

rats. Cancer Res. 1995;55:1277–1282.

31 Hibasami H, Yamada Y, Moteki H, Katsuzaki H, Imai K, Yoshioka K, et al. Sesquiterpenes (costunolide and zaluzanin D) isolated from laurel (Laurus nobilis L.) induce cell death and morphological change indicative of apoptotic chromatin condensation in leukemia HL-60 cells. Int J Mol Med. 2003;12:147–151.

32 Chen HC, Chou CK, Lee SD, Wang JC, Yeh SF. Active compounds from Saussurea lappa Clarks that suppress hepatitis B virus surface antigen gene expression in human hepatoma cells. Antiviral Res. 1995;27:99–109.

33 Sheehan M, Wong HR, Hake PW, Malhotra V, O'Connor M, Zingarelli B. Parthenolide, an inhibitor of the nuclear factor-κB pathway, ameliorates cardiovascular derangement and outcome in endotoxic shock in rodents. Mol Pharmacol. 2002;61:953–963.

34 Sheehan M, Wong HR, Hake PW, Zingarelli B. Parthenolide improves systemic hemodynamics and decreases tissue leukosequestration in rats with polymicrobial sepsis. Crit Care Med. 2003;31:2263–2270.

35 Patel NM, Nozaki S, Shortle NH, Bhat-Nakshatri P, Newton TR, Rice S, et al. Paclitaxel sensitivity of breast cancer cells with constitutively active NF-κB is enhanced by IkappaBalpha super-repressor and parthenolide. Oncogene. 2000;19:4159–4169.

36 Rivero A, Quintana J, Eiroa JL, Lopez M, Triana J, Bermejo J, et al. Potent induction of apoptosis by germacranolide sesquiterpene lactones on human myeloid leukemia cells. Eur J Pharmacol. 2003;482:77–84.

Exp. Anim. 54(1), 101–105, 2005

—Note—

Malignant NK/T-Cell Lymphoma Associated with Simian Epstein-Barr Virus Infection in a Japanese Macaque (Macaca fuscata)

Juri SUZUKI[1)], Shunji GOTO[1)], Akino KATO[1)], Chihiro HASHIMOTO[1)], Norikatsu MIWA[1)], Satomi TAKAO[2)], Takafumi ISHIDA[2)], Ayumi FUKUOKA[3)], Hiroyuki NAKAYAMA[3)], Kunio DOI[3)], and Koichi ISOWA[4)]

[1)]*Primate Research Institute, Kyoto University, Inuyama, Aichi 484-8506,* [2)]*Graduate School of Science, University of Tokyo, Bunkyo, Tokyo 113-0033,* [3)]*Graduate School of Agricultural and Life Sciences, University of Tokyo, Bunkyo, Tokyo 113-8657, and* [4)]*Japan Bioscience Center Co., Ltd., Kaizu, Gifu 503-0628, Japan*

Abstract: *A case of spontaneous malignant lymphoma in a Japanese macaque (*Macaca fuscata*) was pathologically, etiologically and virologically studied. Nasal cavity was involved in the neoplastic lesions in addition to lymphoid and visceral tissues. Histopathological analyses revealed the presence of neoplastic cells classified into histiocytic Hodgkin-like cells and Reed-Sternberg-like cells. Histiocytic Hodgkin-like cells were CD16+ and CD20+, and the CD16+ cells were also positive for simian Epstein-Barr virus (sEBV)-encoded early RNA transcripts. RS-like cells were negative for CD3, CD16 and CD20. Antibodies to early antigen of sEBV were detected, while antibodies to simian T-cell leukemia virus-1 were negative. The case may correspond to EBV-associated nasal type NK/T-cell lymphoma in humans rather than Hodgkin lymphoma.*

Key words: *Japanese macaques, malignant lymphoma, simian Epstein-Barr virus*

Malignant lymphomas are common neoplasms in non-human primates [1, 9, 30] as in humans. Classification of lymphomas in non-human primates, however, is based only on the morphological features. In humans, Hodgkin lymphoma is distinguished from non-Hodgkin lymphoma by the presence of Hodgkin cells (histiocytic neoplastic cells with noticeable nucleus) and/or multinucleated Reed-Sternberg (RS) cells [2] that are derived from B cells in the germinal center, and moreover by various neoplastic cell markers [7, 24]. Analyses of CD markers also help us to classify non-Hodgkin lymphoma in non-human primates and provide more information about the lymphomagenesis [3, 21, 22]. There has been so far only one report on lymphoma with CD marker analyses for the Japanese macaque (*Macaca fuscata*) [31]. However, histological and etiological information were lacking from that report and a systematic study on primate malignant lymphoma has been awaited.

Certain groups of viruses are tightly associated with

(Received 27 April, 2004 / Accepted 25 August, 2004)

Address corresponding: J. Suzuki, Center for Human Evolution Modeling Research, Primate Research Institute, Kyoto University, Inuyama, Aichi 484-8506, Japan

and participate in lymphomagenesis in non-human primates as well as in humans. Epstein-Barr virus (EBV) classified as a lymphocrypto gamma herpesvirus is an etiological agent of lymphoproliferative disorders including Burkitt's lymphoma and infectious mononucleosis in humans [26, 33]. Recent studies on malignant lymphoma have revealed that EBV contributes to the development of Hodgkin and non-Hodgkin lymphoma including T-cell lymphomas such as NK/T-cell lymphoma [4, 5]. Virus isolates relevant to human EBV have been found in non-human primates and are called simian EBV (sEBV) [18]. The sEBV is well known to play an important role in oncogenesis in macaques [16, 25], and 98% of Japanese macaques were seropositive for anti-sEBV viral capsid antigen (sEBV VCA) [11, 12]. One of the primate T-lymphotropic retroviruses, simian T-cell leukemia virus (STLV)-1, has the potential to develop T-cell lymphoma in baboons (*Papio spp.*) [10] and African green monkeys (*Cercopithecus aethiops*) [17], and about 30% of Japanese macaques have been reported to be seropositive for STLV-1 [13, 14].

Recently, a Japanese macaque in our colony was found to have developed a malignant lymphoma and subsequently died. We here report the histopathological, virological and etiological data of the case.

The macaque was born and reared at the Primate Research Institute of Kyoto University. The rearing conditions were described in detail in our previous report [28]. The animal was a male Japanese macaque aged 4.6 years (yrs) and belonged to the Arashiyama troop. Autopsy was performed immediately after the death. Tissues with gross lesions were fixed in 10% formalin solution, embedded in paraffin, sectioned at 5 μm, and stained with hematoxylin and eosin (HE) for histopathological observation.

Immunostaining was performed on paraffin-embedded sections of tissues using antibodies to human CD3 (PS1, Nichirei, Japan) for T-cells, CD16 (NCL-CD16, Novo castra, UK) for NK-cells and CD20 (L26, Nichirei, Japan) for B-cells, which had been confirmed cross-reactive with Japanese macaque's lymphoid antigens on paraffin-embedded sections. Positive signals were visualized by using a Dako LSAB2/HRP kit (DakoCytomation, Japan).

To confirm the presence of sEBV in tumor cells, *in situ* hybridization was performed on sections of tissues using fluorescein-conjugated oligonucleotides (5'-ATCTCCTCCCCAGCATAACCGCTAGGGCAG-3' and 5'-ACCCCCCTCTGTCCGTAACCTC-TAGGCTAG-3') complementary to the portions of the sEBV-encoded early RNA transcripts (sEBERs) that are actively transcribed in latently infected cells. Sections of tissues, axillary and inguinal lymph nodes, of a normal Japanese macaque were used as a control. Signals for sEBERs were visualized by Universal RNA ISH and a DIG-AP detection kit (Nichirei, Japan).

Infection with STLV-1 was monitored by the detection of specific antibody to STLV-1 with an indirect immunofluorescence method. The procedure has been described previously [13]. As for the sEBV infection status, the presence of anti-sEBV VCA antibody and anti-sEBV early antigen (sEA) antibody were used as markers for the sEBV infection and the possible presence of sEBV associated cell proliferative diseases, respectively [22]. P3HR-1 cells [8] treated with 4 mM n-butyric acid (Wako Chem., Japan) and 20 ng/m*l* 12-tetradecanoylphorbol-13-acetate (TPA) (Sigma, USA) for 48 h, and Raji cells [23] treated with 20 ng/m*l* TPA for 5 days were fixed with acetone and used as target antigens of sEBV VCA and sEA, respectively. Fluorescein isothiocyanate-conjugated goat antibody to human immunoglobulins (Medical & Biological Laboratories, Japan) was used to visualize a positive reaction under a fluorescence microscope. The procedure for the detection of plasma antibodies to sEBV VCA and sEA has been described in detail previously [11].

At 3.8 yrs of age, lameness of the left hind limb, high body temperature (39.3°C), increase in white blood cell count (25,600/mm^3) and high concentration of plasma C-reactive protein (CRP) (2.6 mg/dl) were observed. A mass in the left nasal cavity with hemorrhage and rhinorrhea, and swelling of the axial lymph nodes were found at 4.6 yrs of age. Severe anemia (RBC 289 $\times 10^4/mm^3$, hemoglobin 6.2 g/dl, and hematocrit 22.5%), low platelet count ($10 \times 10^4/mm^3$) and high CRP (3.3 mg/dl) and high alkaline phosphatase (1,537 unit/litter) levels were documented before death at the age of 4.6 yrs. A hemogram was not available in the present case.

Gross lesions were characterized by systemic swelling of various lymph nodes (30–70 mm in diameter), a neoplastic mass in the nasal cavity ($30 \times 15 \times 15$ mm) and splenomegaly ($1,250 \times 850 \times 300$ mm).

Histopathological findings of the lymph nodes in-

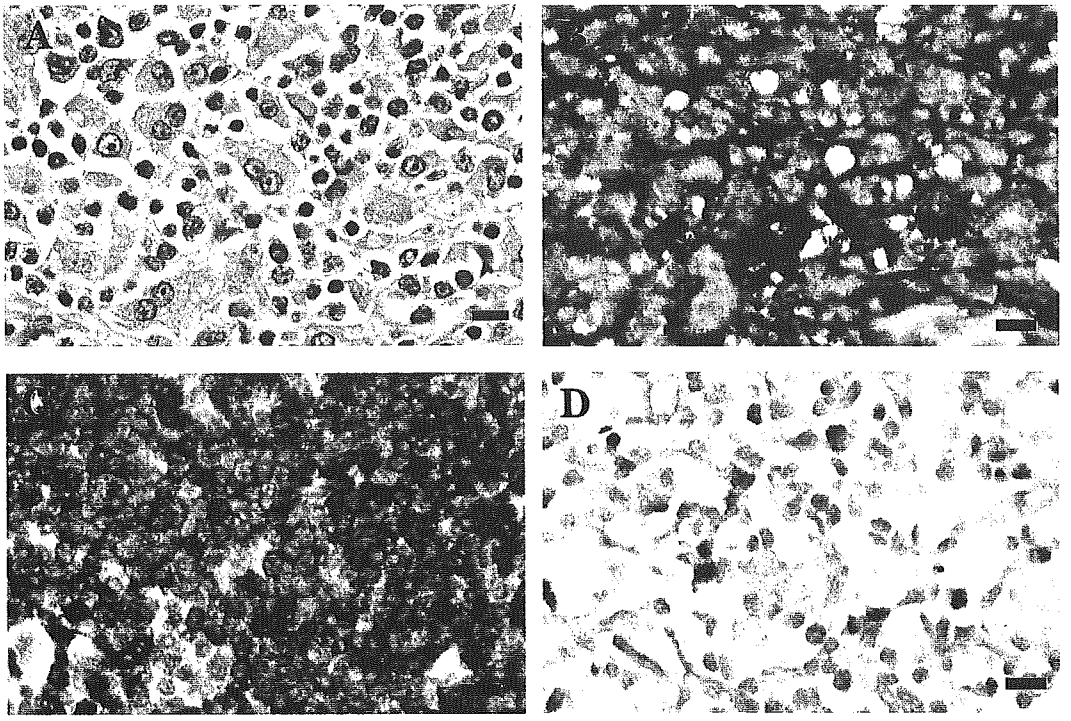

Fig. 1. Neoplastic lesion of the Japanese macaque. Bar = 10 μm. A; HE staining for the mediastinal lymph node. Hodgkin-like histiocytic and RS-like cells are observed. Mononuclear or binuclear RS-like cells are seen in the upper and the central parts. B; CD16+ neoplastic cells in the nasal lesion. Immunohistochemistry C; CD20+ neoplastic cells in the iliac lymph node. Immunohistochemistry. D; sEBER-positive neoplastic cells in the nasal lesion. *In situ* hybridization.

cluding axillary, mediastinal, gastric and iliac were as follows (Fig. 1A). Neoplastic histiocytic cells were proliferated diffusely. Multinucleated RS-like cells having eosinophilic and foamy cytoplasm with polymorphic or kidney-shaped nuclei were scattered in the lesion. Mirror-image in RS-like cells was often observed. Non-neoplastic lymphocytes were diffusely infiltrated into the lesion. Necrosis and fibrosis were apparent in part of the lesion. The lung, liver, spleen and the tumor mass in the left nasal cavity exhibited similar histopathological findings to those in lymph nodes. In the liver, neoplastic cells and non-neoplastic lymphocytes proliferated mainly at the Glisson's sheath.

The histiocytic neoplastic cells were positive for CD16 but negative for CD3 in any organs examined, while CD20-positive histiocytic neoplastic cells were recognized only in the iliac lymph node (Figs. 1B and 1C). RS-like cells were negative for CD3, CD16 and CD20.

Anti-STLV-I antibody was not detected in the case. The titers of anti-sVCA antibody were 1: 160 at 4.6 yrs. Simultaneously anti-sEA antibody was 1: 40. *In situ* hybridization revealed the expression of sEBER in the CD16-positive histiocytic neoplastic cells but not in the RS-like cells of all tissues examined (Table 1, Figs 1B and 1D).

Expression of sEBERs in the neoplastic cells and the concurrent presence of anti-sEA antibody suggest the important role(s) of sEBV in the lymphomagenesis in the present case. Infection of EBV in humans and sEBV in macaques is widely disseminated and causes B-cell malignancies such as Burkitt-type lymphoma. In addition, their frequent involvement even in Hodgkin lymphoma and the non B-cell lymphomas such as NK/T-cell lymphoma has been pointed out [4, 5].

Histopathological observations for the present case revealed that the neoplastic cells were composed of two types. One was round-shaped histiocytic cells (Hodgkin-like cells) with poor to rich cytoplasm and a dark or pale-stained nucleus, and the other was multi-

Table 1. Immunophenotype and sEBV related features of neoplastic cells

	Antibody to			Neoplastic cells* positive for			
	STLV-1	sVCA	sEA	sEBER	CD3	CD16	CD20
	–	1:160	1:40				
Tumor of nasal cavity				+	–	+**	–
Iliac lymph node				+	–	+	+
Liver				+	–	+	–
Spleen				+	–	+	–

*: RS-like cells were negative for all those markers. **: CD16-positive cells were identical to sEBERs-positive cells.

nuclear RS-like cells which are the typical cells of Hodgkin lymphoma in humans [7, 24] and some lymphomas of non-human primates [6, 20]. The ratio of the two cell types varied among the organs where the lesions were observed. Although morphological similarity to human Hodgkin lymphoma was observed in the present case, the majority of neoplastic cells were histiocytic cells with few inflammatory cells in the lesion. Hodgkin lymphoma in humans is characterized by a few RS cells with an inflammatory cell background [15]. These differences suggest that the present case is not comparable with Hodgkin lymphoma in humans.

One of the human non-Hodgkin lymphomas associated with EBV-infection, nasal type NK/T-cell lymphoma [15], manifests nasal involvement of the lesion, prolonged fever, anemia, body weight loss and a high alkaline phosphatase level. Histopathology of nasal type NK/T-cell human lymphoma is characterized by the proliferation of pleomorphic lymphoid cells with the occasional presence of Hodgkin/RS-like cells [27]. The phenotype of the lymphoma cells in the nasal lesion is EBER+, CD2+, CD3-, CD4+, CD8+, CD19-, CD30- and CD56+ [19, 29].

The present macaque case showed nasal involvement and a high alkaline phosphatase level and suffered from severe anemia. Phenotypes of the neoplastic histiocytic cells of the case were sEBER+, CD3-, CD16+ and CD20- in the nasal lesion, and sEBER+, CD3-, CD16+ and CD20+ in the iliac lymph node. For the detection of NK-cells, an antibody to human CD16 was used instead of anti-human CD56 antibody, since the reactivity of a selected anti-human CD56 antibody to monkey cells has not been confirmed. CD16 is also used as another marker to confirm this type of lymphoma [15, 19]. The appearance of CD20+ neoplastic NK/T-cells in the iliac lymph node corresponded to a previous observation in human T-cell lymphoma with an aberrant expression of CD20 and CD79a (both are B-cell markers) [32].

These comparable symptoms and laboratory findings suggest that the present case was a monkey type of nasal NK/T-cell lymphoma rather than Hodgkin lymphoma. The present case, in particular, is highly significant because the number of EBV-associated NK/T-cell lymphoma cases are increasing in humans. Further molecular analyses of the case may establish macaques as an animal model for EBV-associated T-cell or NK/T-cell lymphoma.

Acknowledgments

We are grateful to Prof. W. Mitarnun, Department of Pathology, Faculty of Medicine, Prince of Songkla University, Hat-Yai, Thailand, for his valuable advice. This study was supported in part by the grant in aid for scientific research, MEXT Japan.

References

1. Beniashvili, D.A. 1989. *J. Med. Primatol.* 18: 423–437.
2. Damjanov, I. and Linder, J. 2001. Pathology: A Color Atlas. 1st Japanese ed., Medical Sciences International, Ltd., Tokyo (in Japanese).
3. Feichtinger, H., Kaaya, E.E., Li, S.-L., Putkonen, P., Grünewald, K., Weyrer, K., Offner, F., Biberfeld, G., and Biberfeld, P. 1992. *Verh. Dtsch. Ges. Path.* 76: 189–193.
4. Flavell, K.J. and Murray, P.G. 2000. *J. Clin. Pathol.: Mol. Pathol.* 53: 262–269.
5. Gaal, K., Sun, N.C.J., Herneandez, A.M., and Arber, D.A. 2000. *Am. J. Surg. Pathol.* 24: 1511–1517.
6. Gleiser, C.A., Carey, K.D., and Heberling, R.L. 1984. *Lab. Anim. Sci.* 34: 286–289.
7. Herling, M., Rassidakis, G.Z., Medeiros, L.J., Vassilakopoulos, T.P., Kliche, K.-O., Nadali, G., Viviani,

S., Bonfante, V., Giardini, R., Chilosi, M., Kittas, C., Gianni, A.M., Bonadonna, G., Pizzolo, G., Pangalis, G.A., Cabanillas, F., and Sarris, A.H. 2003. *Clin. Cancer Res.* 9: 2114–2120.
8. Hinuma, Y., Konn, M., Yamaguchi, J., Wudarski, D.J., Blakeskee, J.R., and Grace, J.T. 1967. *J. Virol.* 1: 1045–1051.
9. Holmberg, C.A., Osburn, B.I., Terrell, T.G., and Manning, J.S. 1978. *Am. J. Vet. Res.* 39: 469–472.
10. Hubbard, G.B., Moné, J.P., Allan, J.S., Davis, I.K.J., Leland, M.M., Banks, P.M., and Smir, B. 1993. *Lab. Anim. Sci.* 43: 301–309.
11. Ishida, T., Suzuki, J., and Yamamoto, K. 1993. *Folia Primatol.* 61: 228–233.
12. Ishida, T. and Yamamoto, K. 1987. *J. Med. Primatol.* 16: 359–371.
13. Ishida, T., Yamamoto, K., Kaneko, R., Tokita, E., and Hinuma, Y. 1983. *Microbiol. Immunol.* 27: 297–301.
14. Ishikawa, K., Fukasawa, M., Tsujimoto, H., Else, J.G., Isahakia, M., Ubhi, N. K., Ishida, T., Takenaka, O., Kawamoto, Y., Shotake, T., Ohsawa, H., Ivanoff, B., Cooper, R. W., Frost, E., Grant, F.C., Spriatna, Y., Sutarman, Abe, K., Yamamoto, K., and Hayami, M. 1987. *Int. J. Cancer* 40: 233–239.
15. Jaffe, E.S., Harris, N.E., Stein, H., and Vardiman, J.W. 2001. World Health Organization Classification of Tumours. Tumours of Haematopoietic and Lymphoid Tissues. International Agency for Research of Cancer Press, Lyon, France.
16. Jayo, M.J., Jayo, J.M., Jerome, C.P., Krugner-Higby, L., and Reynolds, G.D. 1988. *Lab. Anim. Sci.* 38: 722–726.
17. Jayo, M.J., Laber-Laird, K., Bullock, B.C., Tulli, H.M., and Reynolds, G.M. 1990. *Lab. Anim. Sci.* 40: 37–41.
18. Levy, J.A., Levy, S.B., Hirshaut, Y., Kafuko, G., and Prince, A. 1971. *Nature* 233: 559–560.
19. Mitarnun, W., Saechan, V., Pradutkanchana, J., Suwiwat, S., Takao, S., and Ishida, T. 2003. *J. Med. Assoc. Thai.* 86: 816–827.
20. Morita, M. 1974. *Primates* 15: 47–53.
21. Mätz-Rensing, K., Pingel, S., Hanning, H., Bodemer, W., Hunsmann, G., Kuhn, E.-M., Tiemann, M., and Kaup, F.-J. 1999 *J. Med. Primatol.* 28: 318–328.
22. Paramastri, Y.A., Wallace, J.M., Salleng, K.J., Wilkinson, L.M., Malarkey, D.E., and Cline, J. M. 2002. *Vet. Pathol.* 39: 399–402.
23. Purvertaft, R.J.V. 1964. *The Lancet* I: 238–240.
24. Rassidakis, G.Z., Medeiros, L.J., Viviani, S., Bonfante, V., Nadali, G.-P., Vassilakopoulos, T.P., Mesina, O., Herling, M., Angelopulou, M.K., Giardini, R., Chilosi, M., Kittas, C., McLaughlin, P., Rodriguez, M.A., Romaguera, J., Bonadonna, G., Gianni, A.M., Pizzolo, G., Pangalis, G.A., Cabanillas, F., and Sarris, A.H. 2002. *J. Clin. Oncol.* 20: 1278–1287.
25. Stowell, R.E., Smith, E.K., España, C., and Nelson, V.G. 1971. *Lab. Invest.* 25: 476–479.
26. Straus, S.E., Cohen, J.I., Tosato, G., and Meier, J. 1993. *Ann. Intern. Med.* 118: 45–58.
27. Suchi, T. 2000. New atlas of malignant lymphoma. Bunkodo, Tokyo.
28. Suzuki, J., Miwa, N., Kumazaki, K., Abe, M., Kamanaka, Y., Matsubayashi, N., Gotoh, S., and Matsubayashi, K. 2001. *J. Vet. Med. Sci.* 63: 361–366.
29. Tao, Q., Ho, F.C., Loke, S.L., and Srivastava, G. 1995. *Int. J. Cancer* 60: 315–320.
30. Terrell, T.G., Gribble, D.H., and Osburn, B.I. 1980. *J. Natl. Cancer Inst.* 64: 561–568.
31. Yanai, T., Sakai, H., Goto, S., Murata, K., and Masegi, T. 2002. *Jpn. J. Zoo Wildl. Med.* 7: 45–51.
32. Yao, X., Teruya-Feldstein, J., Raffeld, M., Sorbara, L., and Jaffe, E.S. 2001. *Mod. Pathol.* 14: 105–110.
33. Zur Hausen, H., Schulte-Holthausen, H., Klein, G., Henle, W., Henle, G., Clifford, P., and Stantesson, L. 1970. *Nature* 228: 1056–1058.

Primates (2005) 46:33–45
DOI 10.1007/s10329-004-0099-3

ORIGINAL ARTICLE

Yuzuru Hamada · Juri Suzuki · Satoshi Ohkura
Seiji Hayakawa

Changes in testicular and nipple volume related to age and seasonality in Japanese macaques (*Macaca fuscata*), especially in the pre- and post-pubertal periods

Received: 10 September 2003 / Accepted: 21 April 2004 / Published online: 30 September 2004

Abstract We investigated, longitudinally and cross-sectionally, age and seasonal change in both the testis and nipple volume of Japanese macaques (*Macaca fuscata*) in relation to concentration profiles of gonadal steroids: testosterone (T) in males and progesterone (P) in females. Testicular volume (TV) and nipple volume (NV) showed rapid growth at puberty, 4.5 and 3.5 years of age in males and females, respectively, but in both sexes there were precocious individuals. The testis as a whole matures at about 10 years of age. TV change is closely related to T concentration profile. The pattern of TV change is composed of maturation and seasonal effects, with individual variation evident mainly in the latter. Some individuals show a simple pattern consisting of one peak in the breeding season (from summer to winter) and one trough in the non-breeding season. Other individuals exhibit a more complicated pattern composed of two or more peaks and troughs before and during the breeding season. The nipple matures at about 7 years but it is difficult to determine the exact maturational age as there are many confounding factors relating to NV. NV shows seasonal fluctuations similar to that of TV. Many animals have periods of substantial growth whereas others do not. The NV in adults from 10 to 25 years does not appear to change much with age, but animals older than 25 years of age have significantly smaller nipples. Seasonal fluctuation in NV mirrors that of the P level. Considered to be controlled by estrogen and P, the NV is a good indicator of the physiological status of reproduction, with its peak about 2 weeks earlier than that of P, that is, at the mid-follicular phase. NV and P level show a similar pattern in pregnancy; from conception, indicated by a P peak, NV and P concentration first decrease, then they increase until peri-parturition and slowly decrease again until the next breeding season.

Keywords Testis · Nipple · Puberty · Japanese macaques · Seasonality

Y. Hamada (✉) · S. Hayakawa
Morphology Section, Primate Research Institute, Kyoto University, 41 Kanrin, Inuyama 484-8506, Japan
E-mail: hamada@pri.kyoto-u.ac.jp
Tel.: +81-568-630521
Fax: +81-568-615775

J. Suzuki
Center for Human Evolution Modeling Research, Primate Research Institute, Kyoto University, Inuyama, Japan

S. Ohkura
Laboratory of Neuro-endocrinology, National Institute of Agrobiological Sciences, Tsukuba, Japan

Introduction

Japanese macaques (*Macaca fuscata*) inhabit the Japan Islands, where a temperate climate prevails and four seasons are clearly demarcated. They show seasonality not only in body weight (Hazama 1964; Suzuki et al. 2000) and nutritional status (Hamada et al. 2003), but also in reproduction (Nozaki 1991). The breeding season is from autumn to winter (from September to February with a peak in November; Nozaki 1994), and the delivery season is from spring to early summer (from March to August with a peak in May; Nozaki 1994). Seasonality in the reproduction of Japanese macaques is predominantly controlled by day length, temperature, and internal calendar (Nozaki 1991). Similar seasonality has been reported in bonnet macaques (Glick 1979). Due to changes in their nutritional status or environmental conditions, female Japanese macaques are reported to experience their menstrual cycle in the non-breeding season (Mori et al. 1997). External genital organs change in size and/or color depending on the season: in males, the testis becomes larger in the breeding season (Nigi et al. 1980) and the skin on the scrotum, inguinal, peri-anal area, and caudal aspects of the thigh become reddish; in females,

the so-called "sexual skin" turns reddish and swells; and in both sexes the facial skin reddens.

Sexually dimorphic traits and their development in primates have attracted much attention (Dixson 1998), especially those in humans (Tanner 1962; Malina and Bouchard 1991). The reproduction-related characters mentioned above, comparable to the secondary sexual characters of humans, develop rapidly with the onset of puberty at about 3.5 years in females and 4.5 years in males (Hamada et al. 1999). In humans, facial, axillary, and pubic hair, breast development, testicular development, and voice changes (Tanner 1962) first occur in the adolescent period and rapidly develop. Some of these characters are also found in Japanese macaques, for example, testicular and musculoskeletal development in males or body proportion changes such as fat accumulation in females. Although the Japanese macaque differs markedly from humans in its strict seasonality in reproduction, it appears that the most striking difference is that women show no morphological changes associated with the menstrual cycle. Knowledge about what and how body part(s) change with age and reproductive maturity may shed light on the evolution of the reproductive system, especially as it relates to social structure. In view of this, the morphological changes associated with the reproductive state in Japanese macaques are of interest.

The purpose of this study was to examine age changes, seasonality, and changes in the physiological activity of reproduction in testis and nipple size (volume) in Japanese macaques. Although we have already preliminarily reported on size (Hamada et al. 1999), we extend analyses here with additional data to examine the relationship of changes in testis and nipple volume with the secretion of reproductive hormones, testosterone (T) for males and progesterone (P) for female. The testis produces sperm and secretes steroid hormones and its volume is considered to reflect the state of these functions (Nigi et al. 1980). Although there are some studies on testicular size variation in macaques (Sade 1964; Glick 1979; Nigi et al. 1980; Matsubayashi and Mochizuki 1982; Matsubayashi and Enomoto 1983; Hamada et al. 1996), the details of seasonal change and individual variation in testicular development have not been examined. The nipple appears to change due to growth, sexual maturation, aging, seasonality, and reproductive physiology (menstrual cycle and pregnancy) as mediated by several hormones and lactation. However, although the nipple has been studied from the perspective of behavior (nipple preference, e.g. Tanaka 1989), size variations have not been studied, except by Terasawa et al. (1983), who analyzed nipple size in rhesus macaques (*M. mulatta*) in the peri-pubertal period.

Methods

We adhered strictly to the "Guide for the Care and Use of Laboratory Primates" of the Primate Research Institute (2003), Kyoto University. Our research protocol was approved by the Animal Welfare and Animal Care Committee.

Subjects for longitudinal observation

We followed the growth and development of 15 subject macaques (5 males and 10 females) from the late juvenile (2 or 3 years) to the late adolescent (7 years) phase. Table 1 lists the dates of birth, periods of study, and numbers of observations. Although some females gave birth, almost all babies were separated from the mother at birth. The period of observation differed with the individual. Five macaques born in the same year were reared in the same group cage, composed of an outdoor (4×6×2.2 m, width × length × height) and an indoor enclosure (3.5×4×2.5 m). Monkey chow was the main food and supplements such as sweet potato or cabbage were given twice a week. The total caloric value of food was determined according to body weight and nutritional status, and water was accessible ad libitum. Somatometrical data were collected every 2 weeks. Subjects were anesthetized with a 2:1 mixture of ketamine hydrochloride (Ketalar 50, Sankyo Co., Ltd., 5 mg/kg body weight) and xyladine (Selactar 2%, Bayer Co. Ltd., 1 mg/kg body weight). Blood was collected by venipuncture every week. Somatometry and blood sampling were made from 11 a.m. after the subjects had fasted overnight.

Subjects of cross-sectional observation

Table 2 lists numbers of cross-sectional data by age and sex. We included longitudinal data points in this tabulation. Subject monkeys other than the longitudinal

Table 1 Subject macaques for the longitudinal measurements

No.	Date of birth	Age during study (years)	Number of observations
Male			
1412	1 June 1992	2.88–6.83	107
1428	25 May 1992	2.90–6.85	106
1439	5 June 1992	2.87–6.82	102
1459	12 March 1993	3.10–7.05	91
1470	5 May 1993	2.95–6.90	91
Total			497
Female			
1433	2 June 1992	4.28–6.83	63
1447	23 June 1992	4.14–6.77	62
1458	31 March 1993	3.47–7.00	81
1460	27 March 1993	3.48–7.01	81
1469	30 April 1993	3.39–6.92	82
1720	2 May 1998	1.95–5.10	68
1729	28 May 1998	1.88–5.02	74
1736	29 May 1998	1.88–5.02	72
1743	9 June 1998	1.85–4.99	73
1744	10 June 1998	1.84–4.99	73
Total			729

Table 2 Number of measurements with age and sex: cross-sectional data

Age (years)	Male	Female	Total
0	3		3
1	9	24	33
2	24	121	145
3	150	123	273
4	137	169	306
5	131	134	265
6	107	104	211
7	10	12	22
8	6	10	16
9–10	6	14	20
11–15	19	24	43
15–20	12	25	37
20–25	12	31	43
25-		14	14
Total	626	805	1,431

subjects were reared in open enclosures of about 800 m^2. During the annual health inspections, which were carried out in autumn, we collected somatometric data and blood samples. We also added data collected arbitrarily in other seasons.

Somatometry

The length (or height, L in millimeters) and width (or diameter, W in millimeters) of the right testis and nipple were measured to the nearest millimeter with a sliding caliper. Assuming an ellipsoid shape for the testis and a cylindrical column for the nipple, we calculated their volumes as follows: testicular volume (TV, milliliters) = $W^2 \times L \times \pi/6{,}000$, in which π stands for the circular constant (Marson et al. 1991), and nipple volume (NV, milliliters) = $W^2 \times L \times \pi/4{,}000$.

Measurement of the concentration of gonadal steroid hormones

We measured the plasma concentration of gonadal steroid hormones, T for males and P for females, to monitor the physiological states of reproduction. In humans, the T level varies within a day with its peak and trough concentrations found in the morning and evening, respectively (Felig et al. 1995). We followed the recommendation that blood be collected at the same time each day (Felig et al. 1995) and sampled animals between 11:00 and 11:30 a.m.

We analyzed the concentration profile of P in the luteal phase to determine the ovulatory menstrual cycle (Nozaki 1991). Although puberty is often determined by menarche, the first menstrual bleeding, as subjects were reared in group cages, that method was not applicable. Reproductive maturation can also be determined by ovulation but the determination of this by direct observation of the ovary requires invasive surgery and anesthesia (Terasawa et al. 1983). The menstrual cycle is often depicted by changes in the concentrations of serum E2 (17β-estradiol), luteinizing hormone (LH), follicle stimulating hormone (FSH), and P. Thus, one of these hormones can represent the cycle in cases where reproductive cycles occur regularly. Although estrogen is known to stimulate breast development at puberty in girls (Mastroianni and Coutifaris 1990), and the development of nipple size in rhesus monkeys is controlled by E2 (Terasawa et al. 1983), estrogen is secreted in a pulse-like surge and high levels occur for only 48 h during mid-cycle (Johnson and Everitt 1995), so frequent sampling is necessary. The secretion patterns of LH and FSH are similarly pulse-like. The period of secretion of P, however, continues for much longer and P of higher than 1 ng/ml is secreted for more than 1 week (in rhesus macaques, Knobil and Hotchkiss 1988; in Japanese macaques, Nozaki 1991). The concentration of P also indicates the maturational status of the ovary because P is secreted directly from here. Therefore, P was regarded as a more appropriate indicator for the present study in which blood samples were collected weekly. Concentrations of plasma T and P were measured with standard radioimmunoassay kits (for details see Suzuki et al. 2000).

Statistical analyses

We examined the age change (maturation) and seasonality of TV and NV, and hormonal profiles, mainly graphically but also with basic statistics using Excel (MicroSoft) and S-Plus 4 (MathSoft). We occasionally smoothed graphs using the loess.smooth function (S-Plus 4, MathSoft). Age was expressed to the order of 0.01 years for analyses, and age and calendar month were used to examine seasonal influences. As the birth dates of subject monkeys were in spring, (range from 12 March to 23 June, average 14 May, see Table 1), age and calendar month and age in years are interchangeable (e.g. the age in years for November at 4 years is about 4.5 years old).

Results

Age change and seasonality in testicular volume (TV)

All cross-sectional data on TV were plotted against age (Fig. 1). TV started its rapid increase at puberty, at about 4.5 years, and matured when the individual became an "adult" at 7 years on average, but there was variation with locality (Nigi et al. 1980; Hamada et al. 1986). Although the variation was considerable after puberty, the maturation pattern of the testis is well depicted by the diagram. In adolescence, considerable seasonal fluctuation was observed. For adults (≥7 years), the median is 42.2 ml, and TV for the 10th and 90th percentiles was 23.9 and 65.8 ml, respectively (Fig. 1a). In the range of TV up to 7 years of age, the maximum was close to the 90th percentile of adults, but the mini-

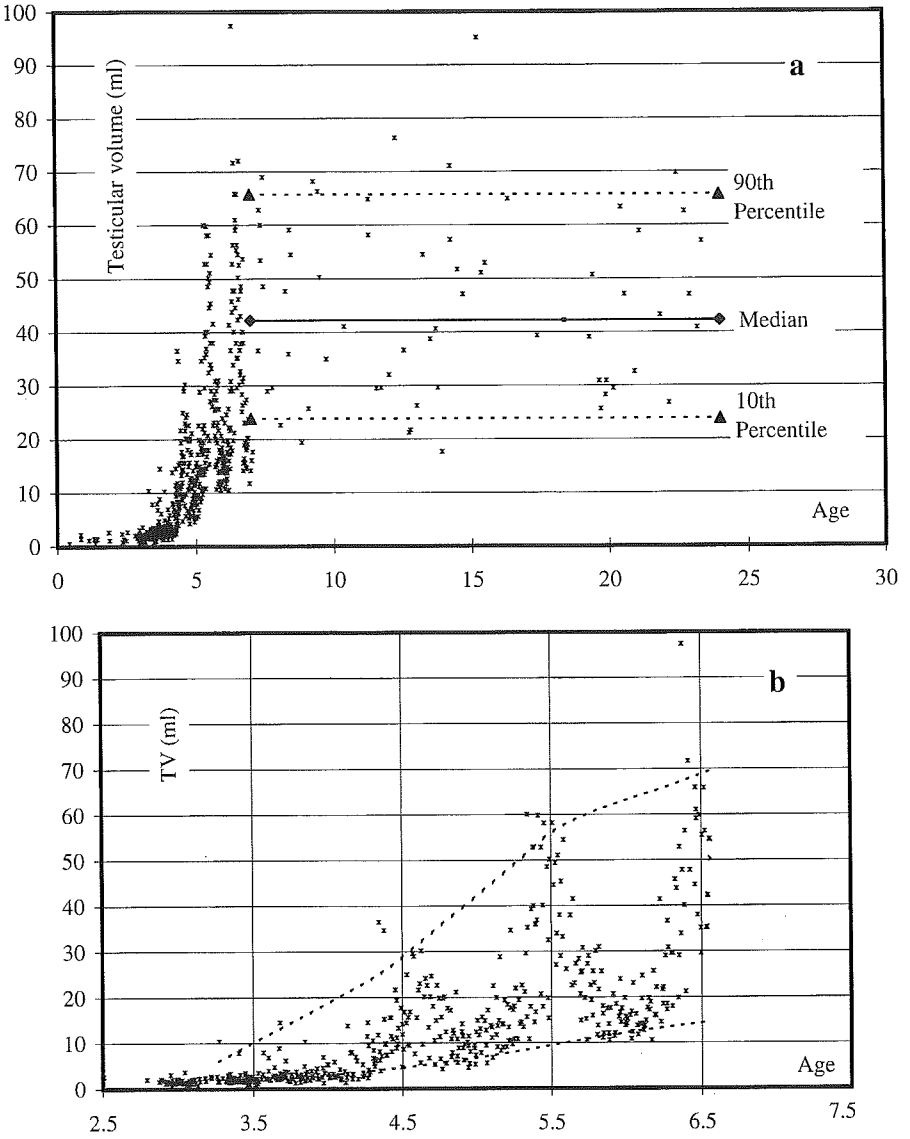

Fig. 1a, b Plots of testicular volume (TV) against age in Japanese macaques. **a** In the adult period, 7–25 years, the median (*line* and *diamonds* at both ends), 10th and 90th percentiles (*dotted lines* and *triangle* at both ends) are superimposed on the diagram. **b** Detail from 2.5 to 7.0 years of age. *Smoothed curves* Connecting peaks and troughs are superimposed

mum (baseline) was smaller than the 10th percentile of adults (Fig. 1b). Therefore, the testis did not appear fully mature at 7 years but it did by about 10 years of age. The oldest monkeys from which we could collect TV measurements were 24 years but we did not note any significant change of TV with age in adults.

Figure 1b shows the details of TV change from the late juvenile to the adolescent period, that is, 3–7 years. TV increased gradually from 3.0 to 4.2 years of age. Although some individuals exhibited a much greater TV than the majority at about 3.5 years (breeding season), a seasonal influence was noted even in these precocious individuals. The TV rapidly increased from 4.2 to 4.6 years (breeding season), to produce the first peak in the graph, and then rapidly decreased to produce a trough at about 5 years (delivery season). Notably, the volume at the trough, the baseline volume (10.36 ml ± 3.39 SD, $n=28$, for subjects aged from 4.90 to 5.10 years), was significantly greater than that at about 4 years of age (3.40 ml ± 1.39 SD, $n=24$, for subjects aged from 3.90 to 4.10 years; $P<0.01$ by t-test).

The testis increased again from the baseline at 5.0 years and achieved a peak of 40–60 ml in the breeding season, whereupon it rapidly decreased again to the trough at about 6.0 years of age in the delivery season. The baseline volume at that age was approximately 15 ml, about 5 ml greater than the previous trough. From 6 to 7 years of age, this seasonal cycle was repeated with greater amplitude, and the baseline volume increased further.

Age changes in TV in the five individuals observed longitudinally are shown in Fig. 2 where the abscissa represents age and calendar month. This graph shows that TV change with age was composed both of seasonal increases and decreases and overall growth. The amplitude of the seasonal cyclical change became greater with age. Because the cyclicity of all individuals was fairly well synchronized, the age change analyzed cross-sec-

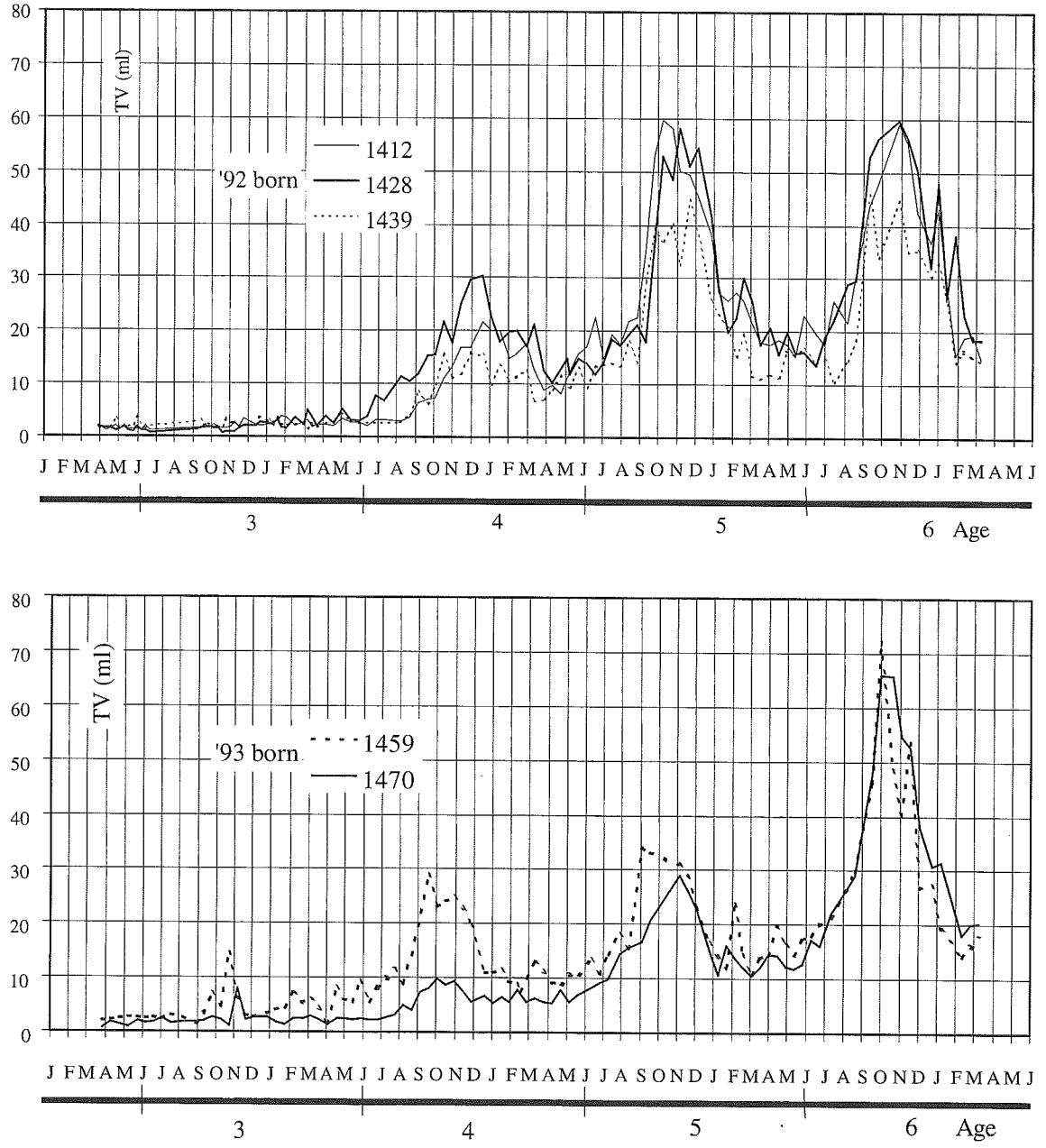

Fig. 2 Longitudinal age change of TV in five males, from 3 to 7 years of age, *top* for subjects born in 1992 and *bottom* for those born in 1993. *Abscissa* is the age and calendar month

tionally preserves the seasonal changes (see Fig. 1b). The dates at peak TV, however, differed somewhat between individuals. Two individuals, numbers 1459 and 1470, showed clear but small peaks in October of the year they were 3, indicating that they were precocious. Before 7 years, their ages at peak TV were slightly younger than those of the other three individuals. Thereafter, the ages of peak TV were similar for all five individuals.

In every individual, peak TV occurred between October and December and then the volume rapidly decreased to its baseline around April. The TV again gradually increased from April, but from mid-September the velocity of increase accelerated until peak TV was reached.

Figure 3 shows the seasonal change of TV in adults of more than 7 years of age, but note that data were not available for every month. As shown by the polynomial regression curve, TV decreased from February to May or June and then it increased in autumn and winter. The maximum volume is about twice that of the minimum.

Testosterone secretion and TV: from the longitudinal analysis of the peri-adolescent period

Figure 4 depicts two examples showing typical relationships between the concentration of serum T (nanograms per milliliter) and TV. Individual 1412 (Fig. 4a)

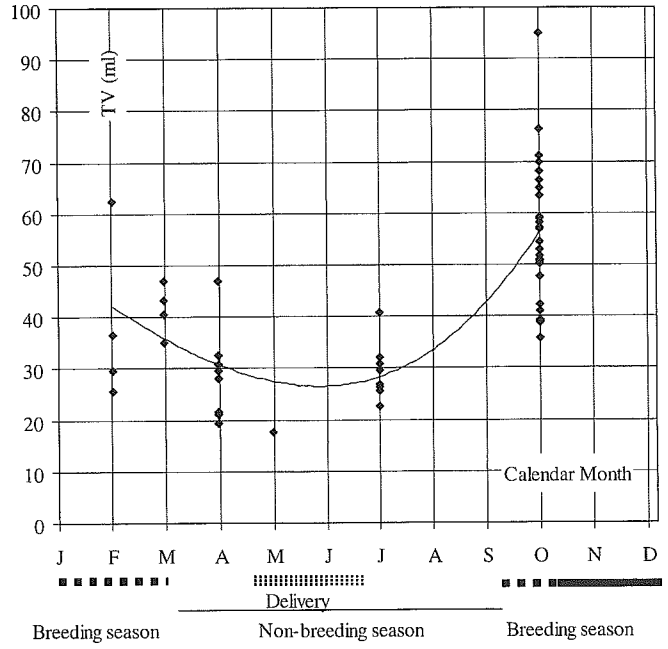

Fig. 3 Seasonal change of TV in adults

shows a simple cyclical pattern with one peak and trough in secretion each year starting from the winter (breeding season) of 4 years of age (ca. 4.5 years). The peak T concentration increased with age: around 4.2 ng/ml at about 4.5 years, 13.5 ng/ml at about 5.5 years, and 14.5 ng/ml at about 6.5 years. The T concentration started to increase rapidly in summer (June–September) and its decrease from the peak concentration was similarly rapid to reach baseline in January or February. The change in TV synchronized well with the T concentration profile, except for the first TV peak, which was later than the T peak by about 1.5 months. TV also started to increase rapidly from 4.5 years, which was concurrent with a rapid increase in T concentration. TV attained its adult mean volume at about 5.5 years of age.

In individual 1459 (Fig. 4b), T secretion occurred early in the year, in both summer and autumn, and there was more than one peak of secretion. At 3 years of age, this individual was clearly precocious to have experienced a significant peak in T secretion in October, with a peak concentration of 4.0 ng/ml, which is comparable to the first peak concentration in individual 1412 at about 4.5 years. Notably, TV temporarily increased in November. At 5 years, there were three peaks in T level, in June, August, and October, the highest of which occurred in August. TV gradually increased from June to August and then, from September, it rapidly increased to the maximum volume of this age, around 30 ml. Although the volume gradually decreased from its peak, it was still more than 20 ml at the end of December. The TV decreased to its baseline of about 10 ml in January and this volume was maintained through to July at 5 years of age.

In the breeding season at 5 years, there were two T peaks at the beginning of July and October, and the TV

Fig. 4a, b Two typical examples showing the relationship between testosterone (*T*) secretion (*dotted line*) and TV change (*solid line*). **a** Simple pattern. **b** Complicated pattern showing secretion in summer

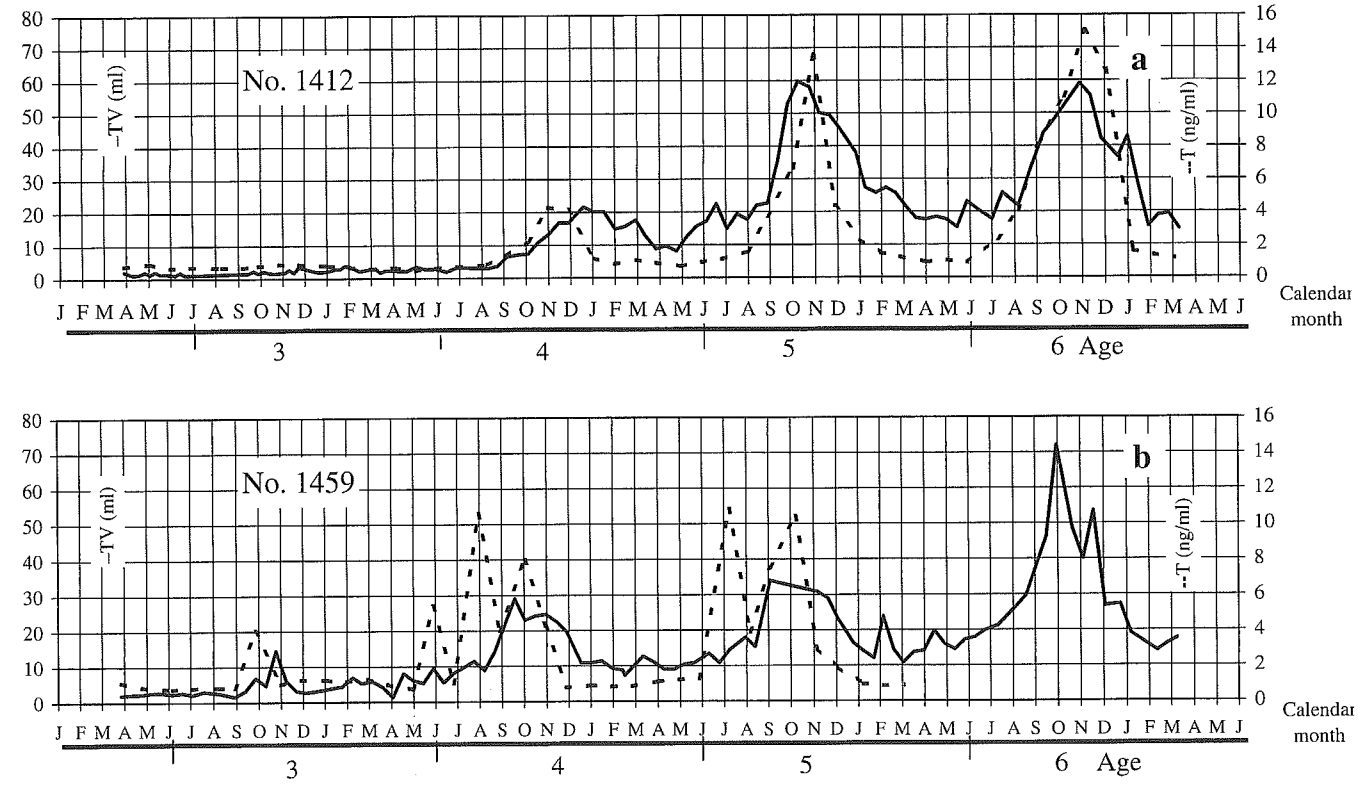

attained a peak volume of around 35 ml, smaller than 40 ml, the median of adults. As TV matured only in the following breeding season, TV development in this individual was retarded. There was a lag (latency period) between T and TV in this individual in the breeding seasons from 3 to 5 years of age when the TV had not yet matured. Of interest is that monkeys reared in the same cage tended to exhibit similar seasonal patterns of TV and T level, that is, numbers 1428 and 1439 were similar to number 1412 and number 1470 was similar to number 1459.

Age change and seasonality of nipple volume

Nipple volume (NV) did not change between birth and 2.5 years (Fig. 5). The nipples grew rapidly from the breeding season of 3 years and matured either in the latter half of adolescence or in the young-adult stage (5–10 years of age). Basic statistics for adults (aged 10–25 years) were mean 4.82 ml (SD = 3.60), median 3.21 ml, 10th and 90th percentiles 0.66 and 8.83 ml, respectively. Thus, the NV in adults was highly variable (Fig. 5a). In adults, there was no significant change in NV with age. Older individuals (≥25 years of age), however, tended to have smaller nipples, with an average of 1.18 ml (SD = 0.96). The difference between means was significant ($P < 0.01$, t-test).

Figure 5b focuses on animals younger than 10 years. The nipple grows slowly from birth to 4 years, to reach a maximum of 1.0 ml. Although some data points are larger than 2.0 ml, the majority fell within the range of 0.5–1.0 ml. A seasonal fluctuation in NV was not evident from this diagram.

We examined the longitudinal age changes in NV in the juvenile and adolescent periods, from 2 to 7 years of age (Fig. 6). With the exception of individual 1447, the graphs of the other nine animals displayed similar age and seasonal changes. The exceptional subject, number 1447, had large nipples that fluctuated unusually. Subject 1729 was precocious by about 6 months. Our subject females first gave birth between 5 and 6 years of age. The distortions to cyclicity caused by pregnancy and lactation are described later.

Change of NV in early adolescence is represented by the graphs of two typical examples (Fig. 7). Individual 1460 (Fig. 7a) displayed regular cyclicity, with almost the same heights of peak NV and the same amplitude of seasonal fluctuation at 3, 4, and 5 years of age.

Subject 1744's (Fig. 7b) peak NV increased greatly from the fourth to the fifth winter, almost doubling in size, and a seasonal change was also evident. Many of the other subjects exhibited trajectories similar to that of 1744, where the baseline volume increased from 4 years and the growth component was quite large. In the fifth winter, there were two additional peaks in NV both before and after the peak in January, and a NV of greater than 0.8 ml was maintained for nearly 6 months

The relationship between the P concentration profile and NV change

Figure 8 shows the P concentration profile and NV change in early adolescence (no. 1469). The first signif-

Fig. 5a, b Plots of nipple volume (*NV*) against age in female Japanese macaques. **a** In adults from 10 to 25 years of age, median (*line* and *diamonds* at both ends), 10th and 90th percentiles (*dotted lines* and *X* at both ends) are superimposed. **b** Nipple change from juvenile to young adult stages. Smoothed curves connecting peaks and troughs are superimposed

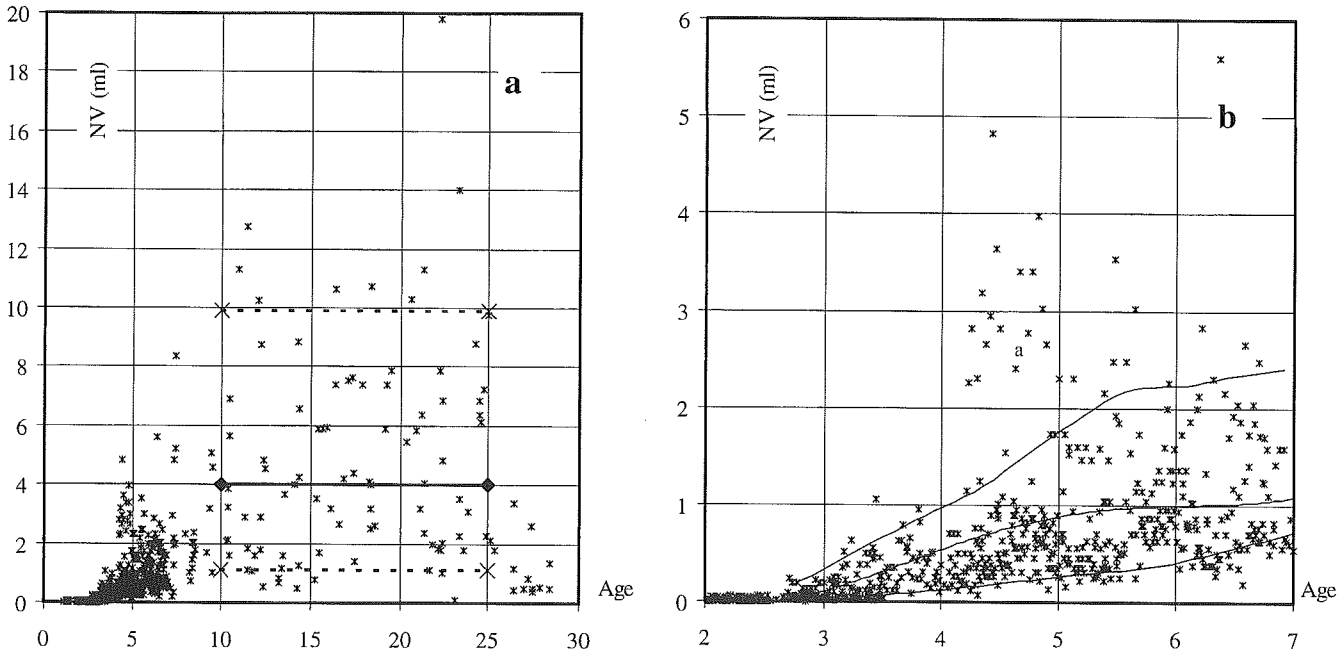

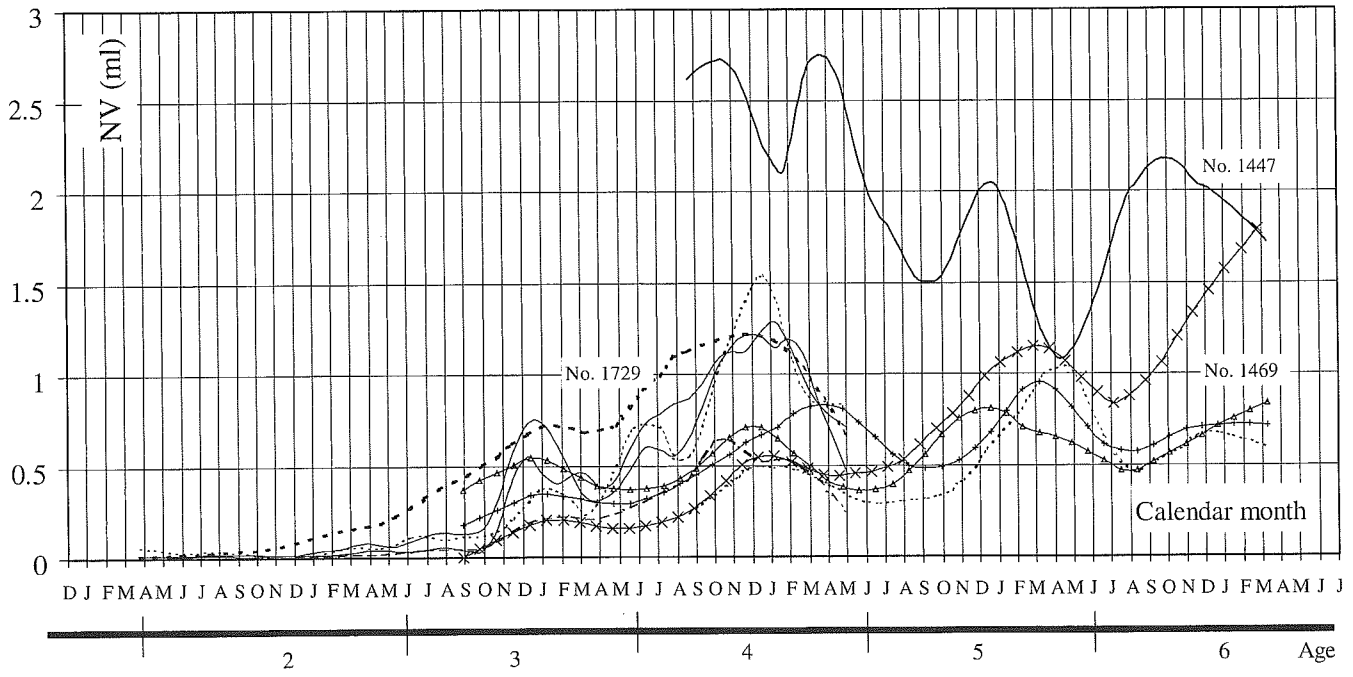

Fig. 6 Longitudinal age change of NV in ten females from 2 to 7 years of age. *Abscissa* is the age and calendar month. The *thick line, dotted thick line*, and *line with X* are the plots for subjects 1447, 1729, and 1469, respectively

icant P peak was found as late as 30 January at 3 years. There was only one peak in that season and NV increased to attain only a low peak, which occurred a little earlier than the P peak.

In the next breeding season, the P level had two major peaks, on 20 November and 18 December, and a smaller peak, little more than 1 ng/ml, occurred on 8 January. The NV started to increase from November and attained its peak in February. Although NV decreased from that peak to a trough in March, it had increased again, despite fluctuations, to 0.6 ml on 30 July. The increase in summer was not accompanied by P-level elevation.

In the third breeding season (at 5 years of age), the P level was slightly higher than 1 ng/ml in October, and then it suddenly increased to its peak on 12 November. We believe that the individual conceived around that date. The NV decreased in early autumn until the 3rd of September, but then it started to increase until around the time of conception.

We next examined the relationship between the concentration profile of P and change in NV in two examples from middle to late adolescence, that is, from 4 to 6 years of age (Fig. 9). Individual 1433 (Fig. 9a) experienced three P peaks in the winter when she was 4 years of age (5 December, 9 January, and 6 February), and following these, a lower peak was found on 14 March. In that same breeding season, we observed three peaks in NV on 20 November, 22 January, and 20 February. After the measurement on 18 December, we ought to have taken measurements on 1 January, but we could do so only on 8 January. If we suppose that a peak occurred there, then a peak in P followed a peak in NV by a reasonably regular lag of about 2 weeks.

The next cycle was initiated in November, and the subject conceived at around the time of the first P peak. The NV and P concentration profile followed the pregnancy pattern that is outlined below.

Although subject 1447 was previously described as an exceptional, she did show another typical pattern of P secretion and NV change (Fig. 9b). In this animal's fourth year, NV increased with three peaks on 24 September, 23 October, and 4 December. The P peaks, however, occurred on 12 December and 9 January. At around the time of the first P peak, the subject was considered to have conceived. NV and P levels showed great fluctuations during pregnancy, and the increase in NV in autumn was not accompanied by a P-level increase.

After parturition, P concentration remained below detection level until the middle of November and then four peaks occurred on 4 and 25 December, 22 January, and 19 February. The NV also peaked four times at roughly monthly intervals, on 13 November, 10 December, 15 January, and 12 February. Considering the interval of measurement of both P concentration and NV, a 2-week lag appears reasonable. The average NV over the 4-month breeding season was about 1.80 ml, higher than the baseline volume of about 1.0 ml. The NV increased again from July to attain a peak on 9 September. Thus, NV increased from summer to autumn as it had when the animal was 4 years old. The P peak was found on 26 November and 24 December and the subject conceived at around the time of this second peak.

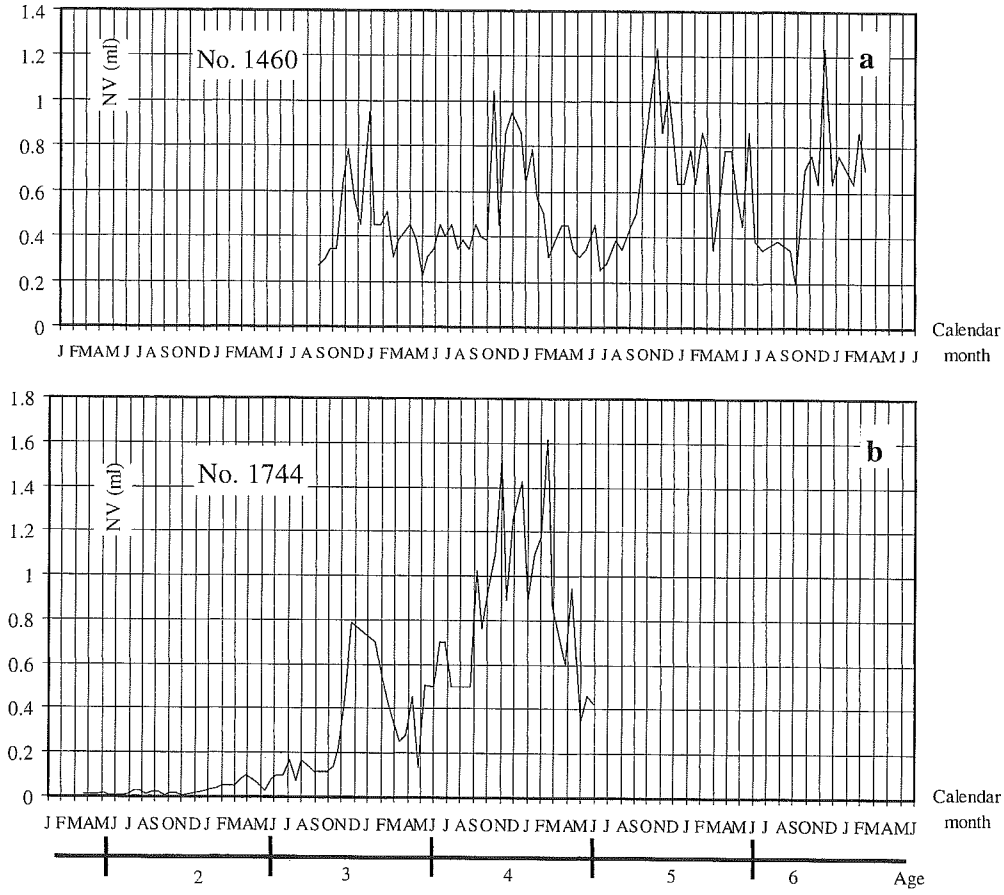

Fig. 7a, b Two examples showing the age change pattern of NV **a** for number 1460: a simple cyclic pattern where the baseline volume does not change with age, and **b** for number 1744: a pattern showing seasonal cyclicity and growth

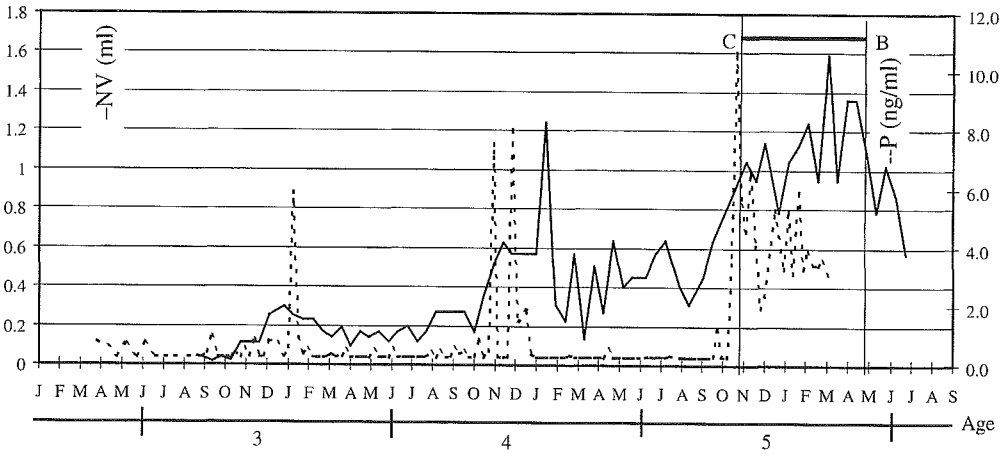

Fig. 8 Age change of NV (*solid line*) and the secretion profile of progesterone (*P*, *dotted line*) in a female subject from the juvenile to the middle of her adolescent period. At 5 years of age this subject became pregnant. In the diagram, *C* (estimated conception), *B* (parturition), and the *thick line* (pregnancy) delineate the pregnancy-related changes

The influence of reproduction on NV: pregnancy pattern

NV change over the period of pregnancy was examined using the P concentration profile for the determination of the day of conception (see Suzuki et al. 2000). The subject depicted in Fig. 8 exhibits the general trend. She conceived in November at 5 years of age and, at that time, NV was already on the increase, as it had been since summer. In many cases, the NV did not show any outstanding characteristics such as a peak or trough on the day of conception. From the P concentration profile, we determined that many subjects conceived during the first or second peak of concentration.

After conception, although NV temporarily decreased, it gradually increased, despite fluctuations, with the advance of pregnancy (see the latter half of 5 years in Fig. 9a and the latter half of 4 years in Fig. 9b). The subject delivered around the time when NV had attained its maximum or second maximum peak in the birth season. After parturition, NV decreased slowly from spring to autumn with fluctuation until it started to follow the menstrual cycle. The concentration profile of

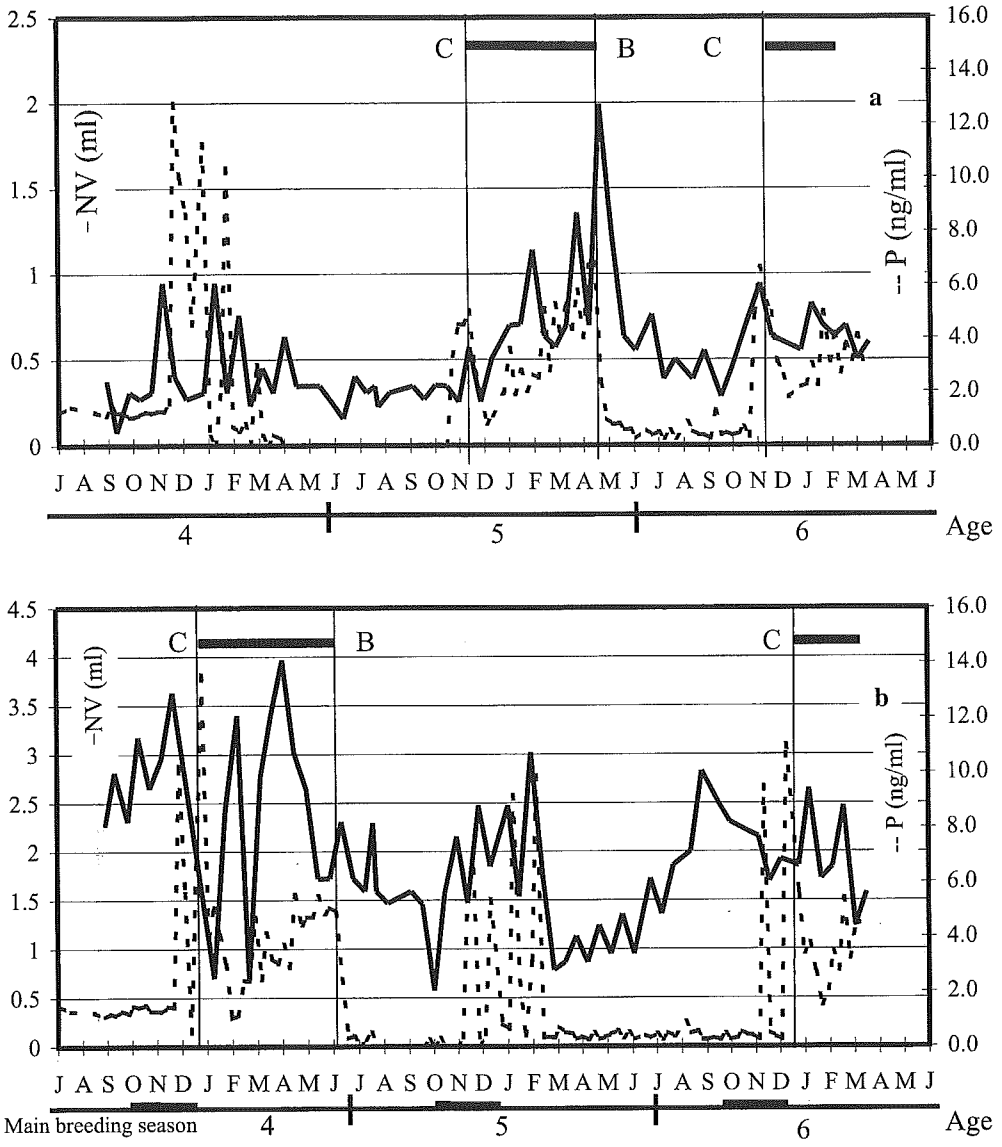

Fig. 9a, b Two examples showing the relationship between the age changes in NV (*solid line*) and the secretion profile of progesterone (*dotted line*). **a** Number 1433; **b** number 1447. *C* (estimated conception), *B* (parturition), and the *thick line* (pregnancy) delineate pregnancy-related changes

P followed almost exactly the change in NV from conception to parturition, but the secretion of P ceased from just after parturition until the next breeding season.

The infant of subject 1469 suckled from its mother for more than 1 year after birth, and the NV graph of this subject increased substantially (Fig. 6). In contrast, the other four subjects in Fig. 6 exhibited the same cycle in the 7th year of life as that found in the previous year. Thus, although NV appeared to increase due to suckling, the exact effect of suckling, especially the cumulative effect, on NV is left for future study.

Discussion

Development and seasonality of the testis in Japanese macaques

The outline of testicular development in Japanese macaques is as follows: the testis starts its rapid increase in size at puberty during the breeding season when animals are about 4.5 years old (e.g. Nigi et al. 1980; Matsubayashi and Mochizuki 1982). There is considerable variation with locality (Hamada et al. 1986) and nutritional status (Hamada et al. 1999) but, on the whole, the testis matures at about 10 years of age (Matsubayashi and Mochizuki 1982). Although the number of subjects was limited, TV did not show age-related changes after reaching maturation. Some animals that grew faster than average in physical dimensions (e.g., body weight) were precocious and showed a small temporal TV increase 1 year earlier. Male long-tailed macaques show a tendency of "catch-up" testicular development, that is, the later the testis starts pubertal development, the faster it develops (Meussy-Dessolle and Dang 1985). We did not, however, find any such significant "catch-up" in the present study.

The TV in Japanese macaques shows a strict seasonality, with an increase before and during the breeding season and a rapid decrease at the end of the season. The